Accepted Manuscript

Geological Society, London, Special Publications

Impact of sea level fluctuations on the sedimentation patterns of the SE African margin: Implications for slope instability

Aaron Micallef, Aggeliki Georgiopoulou, Andrew Green & Vittorio Maselli

DOI: https://doi.org/10.1144/SP500-2019-172

Received 30 September 2019
Revised 14 November 2019
Accepted 20 November 2019

To cite this article, please follow the guidance at https://www.geolsoc.org.uk/onlinefirst#how-to-cite

Impact of sea level fluctuations on the sedimentation patterns of the SE African margin: Implications for slope instability

Aaron Micallef[1,2], Aggeliki Georgiopoulou[3],
Andrew Green[4] and Vittorio Maselli[5]

[1]Marine Geology & Seafloor Surveying, University of Malta, Malta

[2]Helmholtz Centre for Ocean Research, GEOMAR, Kiel, Germany

[3]School of Environment and Technology, University of Brighton, UK

[4]Geological Sciences, University of KwaZulu-Natal, South Africa

[5]Department of Earth and Environmental Sciences, Dalhousie University, Canada
Corresponding author (email: aaron.micallef@um.edu.mt)

Abstract: The sheared-passive margin offshore Durban (South Africa) is characterised by a narrow continental shelf and steep slope hosting numerous submarine canyons. Supply of sediment to the margin is predominantly terrigenous, dominated by discharge from several short but fast-flowing rivers. IODP Expedition 361 provides a unique opportunity to investigate the role of sea level fluctuations on the sedimentation patterns and slope instability along the South African margin. We analysed >300 sediment samples and downcore variations in P-wave, magnetic susceptibility, bioturbation intensity, and bulk density from site U1474, as well as regional seismic reflection profiles to: (i) document an increase in sand input since the mid-Pliocene; (ii) associate this change to a drop in sea level and extension of subaerial drainage systems towards the shelf-edge; (iii) demonstrate that slope instability has played a key role in the evolution of the South Africa margin facing the Natal Valley. Furthermore, we highlight how the widespread occurrence of failure events reflects the tectonic control on the morphology of the shelf and slope, as well as bottom current scour and instability of fan complexes. This information in important to improve hazard assessment in a populated coastal region with growing offshore hydrocarbon activities.

Introduction

Borehole U1474, drilled in the Natal Valley during IODP expedition 361 in 2016, provides a unique opportunity to investigate sedimentation patterns and slope instability in the south-east African passive continental margin offshore Durban, KwaZulu-Natal, South Africa. The margin is relatively underexplored, yet it remains of interest in view of its unusual geological setting. It consists of one of the narrowest continental shelves in the world (Shepard, 1963), which passes basinward into a steep slope that hosts large-scale mass wasting deposits, including submarine canyons (Wiles et al., 2013), slumps (Dingle and Robson, 1985) and big (up to 34,000 km^2) landslides (Martin, 1984; Goodlad, 1986). The area is considered susceptible to slope instability due to the preconditioning of the slope by weakly consolidated siltstone layers (Green et al., 2008), coupled to the large quantities of sediment delivered by numerous fast-flowing rivers from the hinterland (Martin, 1987) and undercutting by strong bottom current activity (Ben-Avraham et al., 1994; Niemi et al., 2000; Wiles et al., 2013). The hazard associated with such processes needs to be quantified in consideration of the proximity to coastal cities and undersea cable infrastructure (Chattopadhyaya, 2018), as well as the recently approved oil and gas exploration activities in the area (Myeni, 2019). Here we combine borehole data from IODP Site U1474 with seismic reflection profiles to understand which processes control sediment supply in the southern Natal Valley, to determine the causes of slope instability, and to evaluate how mass wasting processes affect the evolution of the south-east African margin facing the Indian Ocean.

Regional setting

The Natal Valley developed during the Early Cretaceous (Goodlad et al., 1982; Watkeys and Sokoutis, 1998) following the break-up of Gondwana. The Natal Valley is a sediment filled basin where open marine sedimentation has been recorded since the Late Cretaceous (Davison and Steel, 2017). Uplift of the hinterland started during the Oligocene and triggered an increase in the rate of sediment supply (Said et al., 2015), favouring the formation of thick sequences of deep-water deposits, at places eroded and re-worked by ocean bottom circulation (Niemi et al., 2000; Wiles et al., 2013). The Natal Valley is bordered to the west by the Agulhas-Falkland Fracture Zone (Fig. 1), which represents a 1,200 km long right-lateral strike-slip fault zone that evolved between the South American and African plates during the Early Cretaceous break-up. To the north and east, the Natal Valley is confined by the Mozambique Ridge (Fig. 1), a large igneous province of oceanic origin (Sinha et al., 1981; Fischer et al., 2017).

The South African margin facing the Natal Valley (Fig. 1) is characterised by a narrow continental shelf, up to 10 km wide, which abruptly ends on a steep escarpment associated to the Agulhas-Falkland Fracture Zone (Ben-Avraham et al., 1993). The Natal Valley is a NE-SW elongated bathymetric low that reaches a modern water depth of 4,000 m. South-westward, the Natal Valley opens and deepens into the Transkei Basin (Fig. 1), while the Agulhas Plateau rises to 2,000 m from the abyssal plain farther to the south-west (Fig. 1). The western slope of the Natal Valley hosts a number of submarine canyons that have variable depth and width, and that often indent the shelf. Several submarine landslides have been also recognised along the South African margin, including the Agulhas Slump, presumably the world's largest submarine landslide (Dingle, 1977).

Sediments to the Natal Valley are delivered by numerous steep and fast-flowing rivers, such as the Tugela River, which are sourced from an area of high topographic relief (>3,000 m) that is currently characterised by a sub-tropical high-rainfall climate. The main focus of sedimentation occurs within the Tugela Cone, an asymmetric delta-fan complex seaward of the Tugela River (Goodlad et al., 1982). Additional clastic input is derived from the Limpopo and Zambezi rivers located farther to the north, as well as by deep-water ocean circulation, which creates a series of elongated sediment drifts along the slopes bordering the Natal Valley, the Agulhas Plateau and the Mozambique Ridge (Niemi et al., 2000).

The modern circulation of the south Indian Ocean is characterised by two main currents (Schott et al., 2009). The Agulhas Current is a warm and saline surface current that represents the western boundary current of the Indian Ocean and affects the entire water column (Lutjeharms, 2006). The current flows along the continental shelf of Mozambique and South Africa, reaching velocities of up to 1.5 m/s (Bryden et al., 2005), and contributing to the dispersal of surface sediments. When reaching the Atlantic Ocean, the Agulhas Current retroflects, flowing back to the south Indian Ocean (Toole and Warren, 1993; Lutjeharms, 2006). The Agulhas Undercurrent carries the North Atlantic Deep Water and flows north-eastwards along the slope at water depths of 1000-2900 m and 11-60 km offshore Durban (Lutjeharms and Ansorge, 2001; Beal, 2009). IODP Site U1474 is located in an area where the Agulhas Current is particularly stable due to the confinement generated by the steep slope (Simon et al., 2015). The IODP site is not affected by the Agulhas Undercurrent.

Data and methods

Seismic reflection data

The seismic reflection data presented here comprise legacy, reprocessed, migrated stack 2D seismic reflection profiles obtained for petroleum exploration during the mid-1970s (Hicks and Green, 2016). The single-channel 2D seismic profiles were obtained from the Petroleum Agency of South Africa (PASA) in SEG-Y format and imported into IHS Global Inc. Kingdom Advanced V2015.0. Digital well shoot/velocity data from the Jc-D1 well were utilised by PASA to define two-way time vs. measured depth (m) in order to tie well data to the seismic data (Hicks and Green, 2016).

Borehole data

IODP Site U1474 is located in the northern portion of the Natal Valley (Latitude: 31°13.00’ S; Longitude: 31°32.71’ E, Fig. 1; (Hall et al., 2017)) at a water depth of 3,045 m below sea level. 317 sediment samples were obtained from holes A, B and F, which were processed with a Malvern Mastersizer 3000™ to determine grain size distribution. Downcore variations in bioturbation intensity were measured during the expedition, whereas changes in P-wave velocity, magnetic susceptibility and bulk density were determined using a multi-sensor core logger with a Bartington Instruments MS2C system and a GRA bulk densitometer (Hall et al., 2017).

Results

Seismic reflection data

Two principal seismic facies can be interpreted from the seismic reflection profiles (Fig. 2, 3):

- Facies A (light grey in Fig. 2c, 3c): high amplitude, sub-parallel, continuous reflectors; in view of their correlation with drift deposits, formed by the northward flowing Agulhas Undercurrent at IODP Site U1474 (Niemi et al., 2000; Hall et al., 2017), and their seismic geometry (most notably the continuous and flat-lying nature of the reflectors, which bear strong similarity to those recognised as contouritic sheeted drift deposits (Nielsen et al., 2008; Rebesco et al., 2014)), we interpret facies A as contouritic drift deposits;

- Facies B (dark grey in Fig. 2c, 3c): acoustically chaotic facies with prominent high amplitude reflectors occurring in association with upslope rotated blocks, which we interpret as mass transport deposits (MTD) (Dingle, 1977).

Profile P1 is perpendicular to the shoreline and located to the south-west of the Tugela Cone (Fig. 1, 2). The continental slope and rise consist of facies B that is up to 1 s two-way travel time (TWTT) thick. The high amplitude reflectors correspond to glide plains and allow identification of a number of rotated blocks (Fig. 2). The abyssal plain consists of up to 1 s TWTT thick facies A, which intersects IODP Site U1474, and which is underlain by facies B (Fig. 2). The base of facies A corresponds to the O reflector of Niemi et al. (2000).

Profile P2 is located south of, and partly intersects the southern edge of, the Tugela Cone (Fig. 1, 3). The continental slope comprises up to 1.5 s TWTT of facies B, which extend into the abyssal plain. Here, facies B is overlain by an alternating sequence of facies A with facies B (Fig. 3). The top of the sequences consists of facies B.

Borehole data

Sediments at IODP Site U1474 are 60% terrigenous (predominantly clay) and 40% biogenic (predominantly nannofossils) (Hall et al., 2017). We identify four units based on the physical logs, grain size distribution and bioturbation intensity (Fig. 4):

a) Unit 1 comprises the top 3 m. It is marked by a sharp drop and then an increase in P-wave velocity, similar to the magnetic susceptibility, and a peak in the D10 grain size fraction (Fig. 4). Bioturbation intensity is moderate. Unit 1 is likely the Holocene cover and is the equivalent of unit 1 of the shipboard description (Hall et al., 2017).
b) Unit 2 is observable between 3 and 33 m below sea floor (bsf). Based on the age model, the base of the unit has an age of 900 ka (Fig. 5), which corresponds to the late Pleistocene. In unit 2 there is an overall grain size increase (seen in the high D90 grain sizes), erratic bulk density, and consistent P-wave velocity (Fig. 4). This interval is weakly bioturbated.
c) Unit 3 covers the depths 33 – 141 m bsf and its base has an age of 3.75 Ma (Fig. 5), which corresponds to the mid-Pliocene (P reflector of Niemi et al. (2000)). In this unit we observe the most frequent sand input. Bioturbation is moderate to high, and there is an apparent cyclicity, particularly in the P-wave velocity and the magnetic susceptibility logs (Fig. 4). It is likely that the cyclicity is not restricted to unit 3, as similar patterns in these two logs can be seen deeper in the stratigraphy. However, the cyclicity in unit 3 is more pronounced, possibly due to the presence of more sand units that amplify the signal in P-wave velocity and the magnetic susceptibility as they respond to the presence of (terrigenous) ferro-manganese minerals. Based on the age model, the cycles appear to be have a duration of ~400 ka (Fig. 4).

d) Unit 4 extends from 141 m bsf to the base of the core at 254 m bsf. It is characterised by thinner and less frequent sand beds, and increased bioturbation that becomes more intense with depth. Unit 4 is a finer grained sequence compared to unit 3 (Fig. 4).

Discussion and Conclusions

Source of sediment in IODP Site U1474

Sediment recovered from IODP Site U1474 comprises a combination of terrigenous and hemipelagic sediments. The terrigenous clays are likely sourced by the main drainage systems of the KwaZulu-Natal coast (Martin, 1987; Ziegler et al., 2013; Simon et al., 2015). Low rates of sedimentation characterise much of the sequence (3.7 cm/ka; (Hall et al., 2017)) and the occurrence of thin sand beds point to a sediment supply from the distal part of the slope turbidite system of the northern Natal Valley. However, since IODP Site U1474 is located on a drift deposit (Fig. 2, 3), we cannot exclude that coarse-grained layers may be related to bottom current activity.

Control of sand input to drift sequence in IODP Site U1474

The major drift bodies in the vicinity of the Natal Valley started to develop at the Eocene-Oligocene boundary, in correspondence with the onset of cold, abyssal current circulation (Hall et al., 2017). In IODP Site U1474, a higher input of sand is observed from the mid-Pliocene. In southern Africa, this period corresponds to a significant drop of relative sea level from >300 m down to -200 m compared to present sea level (Siesser and Dingle, 1981). From the mid-Pliocene onwards, sea level fluctuated between -200 m and 0 m (Siesser and Dingle, 1981). We therefore suggest that the higher sand input from the mid-Pliocene onwards is a result of the extension of subaerial drainage systems across the continental shelf and upper slope, and the discharge of terrigenous sediments directly onto the slope, particularly via submarine canyons. In view of this, we infer that the sand intervals are more likely to be turbidites than contourite structures. We interpret the ~400 ka cyclicity in the P-wave velocity and the magnetic susceptibility logs as a sedimentary signature of Milankovitch-type eccentricity of the Earth's orbit (Hays et al., 1976).

Causes of margin-scale slope instability

The seismic reflection profiles show that slope instability has played a key role in the evolution of the South African margin facing the Natal Valley. We attribute the widespread occurrence of slope failure signatures in the continental slope, rise and abyssal plain to the following factors:

a) Shelf width: The shelf is relatively narrow and shallow. It is considered a morphologically inherited feature of the initial shearing phase during margin development (Martin, 1984). Fluvial sediments delivered here were not stored on the shelf, but readily moved offshore, especially during sea level lowstands. The 100 m deep shelf break is always shallower than the Pleistocene lowstands (Compton, 2011), and hence no accommodation space was available for lowstand deltas, resulting in strong loading of the upper slope during glaciations, and their subsequent failure. In addition, in view of the narrow shelf, it is likely that rivers could have delivered sediments directly to the continental slope in places, supplying turbidity currents.
b) Steep continental slope and bottom current activity: The continental slope, due to preservation of a Miocene/Pliocene shelf edge wedge, is over-steepened in the upper

portions (Green et al., 2007). Any undercutting of the lower continental slope would quickly evolve into retrogressive failures, which we observe in profiles P1 and P2 (Fig. 2, 3). We suggest that undercutting of the lower continental slope by vigorous bottom current activity, particularly the Agulhas Undercurrent, is an important cause of slope instability. Wiles et al. (2013) have reported similar scouring by North Atlantic Deep Water in the lower Tugela Cone.

c) Uplift: Starting from the Oligocene, hinterland uplift enhanced slope instability and shedding of large quantities of sediment to the slope (Said et al., 2015; Hicks and Green, 2017). Seismic triggers might also have been important during this time considering that the study site has been recently affected by earthquakes up to 5 ML in magnitude (Wiles et al., 2014).

d) Fan complex instability: Profile P2 shows that, in comparison to profile P1, mass transport deposits are more common and extensive in the vicinity of the Tugela cone, which indicates that rapid accumulation of sediments in this fan complex lead to widespread mass wasting until recently. Hicks and Green (2017) document continued mass wasting and canyon development just north of the study site, focused along the Tugela Cone through Oligocene to Pleistocene times.

Future work

We have demonstrated that sea level fluctuations and slope instability play an important role in the evolution of the sheared-passive margin offshore Durban. Investigation of the margin with higher resolution geophysical techniques will allow us to better understand the style, spatial distribution, preconditioning and triggering factors of slope failures, and to quantify the hazard that they pose.

We thank Jason Chaytor, Samantha Clarke and an anonymous reviewer for their insightful comments.

References

Beal, L.M., 2009. A time series of Agulhas Undercurrent transport. Journal of Physical Oceanography, 39(10), 2436-2450.

Ben-Avraham, Z., Hartnady, C.J.H., Malan, J.A., 1993. Early tectonic extension between the Agulhas bank and the Falkland Plateau due to rotation of the Lafonia microplate. Earth and Planetary Science Letters, 117, 43-58.

Ben-Avraham, Z., Niemi, T.M., Hartnady, C.J., 1994. Mid-Tertiary changes in deep ocean circulation patterns in the Natal Valley and Transkei Basin, Southwest Indian Ocean. Earth and Planetary Science Letters, 121(3-4), 639-646.

Bryden, H.L., Beal, L.M., Duncan, L.M., 2005. Structure and Transport of the Agulhas Current and Its Temporal Variability. Journal of Oceanography, 61(3), 479-492.

Chattopadhyaya, S., 2018. How is Digital Economy of Africa Enabled by Subsea Cable Connectivity, https://www.submarinenetworks.com/en/insights/how-is-digital-economy-of-africa-enabled-by-subsea-cable-connectivity, 2019.

Compton, J.S., 2011. Pleistocene sea-level fluctuations and human evolution on the southern coastal plain of South Africa. Quaternary Science Reviews, 30(5-6), 506-527.

Davison, I., Steel, I., 2017. Geology and hydrocarbon potential of the East African continental margin: a review. Petroleum Geoscience, 24(1), 57-91.

Dingle, R.V., 1977. The anatomy of a large submarine slump on a sheared continental margin (SE Africa). Journal of Geological Society of London, 134, 293-310.

Dingle, R.V., Robson, S., 1985. Slumps, canyons and related features on the continental margin off East London, SE Africa (SW Indian Ocean). Marine Geology, 67(1-2), 37-54.

Dorschel, B., Jensen, L., Arndt, J.E., Brummer, G.J., de Haas, H., Fielies, A., Franke, D., Jokat, W., Krocker, R., Kroon, D., Pätzold, J., 2018. The Southwest Indian Ocean Bathymetric Compilation (swIOBC). Geochemistry, Geophysics, Geosystems, 19(3), 968-976.

Fischer, M.D., Uenzelmann-Neben, G., Jacques, G., Werner, R., 2017. The Mozambique Ridge: a document of massive multistage magmatism. Geophysical Journal International, 208, 449-467.

Goodlad, S.W., 1986. Tectonic and sedimentary history of the mid-Natal Valley (SW Indian Ocean). PhD, University of Cape Town.

Goodlad, S.W., Martin, A.K., Hartnady, C.J.H., 1982. Mesozoic magnetic anomalies in the southern Natal Valley. Nature, 295, 686-688.

Green, A.N., Goff, J.A., Uken, R., 2007. Geomorphological evidence for upslope canyon-forming processes on the northern KwaZulu-Natal shelf, SW Indian Ocean, South Africa. Geo-Marine Letters, 27, 399-409.

Green, A.N., Ovechkina, M., Uken, R., 2008. Nannofossil age constraints on shelf-edge wedge development: implications for continental margin dynamics, northern KwaZulu-Natal, South Africa. Continental Shelf Research, 28, 2442-2449.

Hall, I.R., Hemming, S.R., LeVay, L.J., Barker, S., Berke, M.A., Brentegani, L., Caley, T., Cartagena-Sierra, A., Charles, C.D., Coenen, J.J., Crespin, J.G., Franzese, A.M., Gruetzner, J., Han, X., Hines, S.K.V., Jimenez Espejo, F.J., Just, J., Koutsodendris, A., Kubota, K., Lathika, N., Norris, R.D., Periera dos Santos, T., Robinson, R., Rolinson, J.M., Simon, M.H., Tangunan, D., van der Lubbe, J.J.L., Yamane, M., Zhang, H., 2017. Site U1474. In: I.R. Hall, S.R. Hemming, L.J. LeVay, the Expedition 361 Scientists (Eds.), Proceedings of the International Ocean Discovery Program 361. International Ocean Discovery Program, College Station.

Hays, J.D., Imbrie, J., Shackleton, N.J., 1976. Variations in the Earth's orbit: Pacemaker of the ice ages. Science, 194, 1121-1132.

Hicks, N., Green, A.N., 2016. Sedimentology and depositional architecture of a submarine delta-fan complex in the Durban Basin, South Africa. Marine and Petroleum Geology, 78, 390-404.

Hicks, N., Green, A.N., 2017. A Mid-Miocene erosional unconformity from the Durban Basin, SE African margin: A combination of global eustatic sea level change, epeirogenic uplift, and ocean current initiation. Marine and Petroleum Geology, 86, 798-811.

Lutjeharms, J.R.E., 2006. The Agulhas Current. Springer-Verlag, Berlin.

Lutjeharms, J.R.E., Ansorge, I.J., 2001. The Agulhas return current. Journal of Marine Systems, 30(1-2), 115-138.

Martin, A.K., 1984. Plate tectonic status and sedimentary basin in-fill of the Natal Valley (SW Indian Ocean) PhD, University of Cape Town.

Martin, A.K., 1987. Comparison of sedimentation rates in the Natal Valley, south-west Indian Ocean, with modern sediment yields in east coast rivers of Southern Africa. South African Journal of Science, 83, 716-724.

Myeni, G., 2019. Offshore Oil Exploration Gets Green Light, https://zululandobserver.co.za/199022/offshore-oil-exploration-gets-green-light/, 2019.

Nielsen, T., Knutz, P.C., Kuijpers, A., 2008. Seismic expression of contourite depositional systems. Developments in Sedimentology 60, 301-321.

Niemi, T.M., Ben-Avraham, Z., Hartnady, C.J.H., Reznikov, M., 2000. Post-Eocene seismic stratigraphy of the deep ocean basin adjacent to the southeast African continental margin: a record of geostrophic bottom current systems. Marine Geology, 162, 237-258.

Rebesco, M., Hernández-Molina, F.J., Van Rooij, D., Wåhlin, A., 2014. Contourites and associated sediments controlled by deep-water circulation processes: State-of-the-art and future considerations. Marine Geology, 352, 111-154.

Said, A., Moder, C., Clark, S., Ghorbal, B., 2015. Cretaceous-Cenozoic sedimentary budgets of the Southern Mozambique Basin: implications for uplift history of the South African Plateau. Journal of African Earth Science, 109, 1-10.

Schott, F.A., Xie, S.P., McCreary, J.P., 2009. Indian Ocean circulation and climate variability. Reviews of Geophysics, 47, RG1002.

Shepard, F.P., 1963. Submarine Geology (2nd edition). Harper and Row, London.

Siesser, W.G., Dingle, R.V., 1981. Tertiary sea-level movements around southern Africa. Journal of Geology, 89(4), 523-536.

Simon, M.H., Ziegler, M., Bosmans, J., Barker, S., Reason, C.J.C., Hall, I.R., 2015. Eastern South African hydroclimate over the past 270,000 years. Scientific Reports, 5, 18153.

Sinha, M.C., Louden, K.E., Parsons, B., 1981. The crustal structure of the Madagascar Ridge. Geophysical Journal International, 66, 351-377.

Toole, J.M., Warren, B.A., 1993. A hydrographic section across the subtropical South Indian Ocean. Deep-Sea Research Part I, 40, 1973-2019.

Watkeys, M.K., Sokoutis, D., 1998. Transtension in southeastern Africa associated with Gondwana break-up. Special Publications Geological Society of London, 135, 203-214.

Wiles, E., Green, A., Watkeys, M., Jokat, W., Krocker, R., 2013. The evolution of the Tugela canyon and submarine fan: a complex interaction between margin erosion and bottom current sweeping, southwest Indian Ocean, South Africa. Marine and Petroleum Geology, 44, 60-70.

Wiles, E., Green, A., Watkeys, M., Jokat, W., Krocker, R., 2014. Anomalous seafloor mounds in the northern natal valley, southwest Indian Ocean: implications for the east African rift system. Tectonophysics, 630, 300-312.

Ziegler, M., Simon, M.H., Hall, I.R., Barker, S., Stringer, C., Zahn, R., 2013. Development of Middle Stone Age innovation linked to rapid climate change. Nature Communications, 4(1), 1905.

Figure captions

Fig. 1: Location map and regional physiography. Bathymetric data from Dorschel et al. (2018). Red start denotes location of IODP Site U1474.

Fig. 2: Seismic reflection profile P1 and its interpretation. Location of inset in Fig. 1. Bathymetric data used in inset sourced from Dorschel et al. (2018). Location of IODP Site U1474. TWTT = two-way travel time. MTD = mass transport deposit.

Fig. 3: Seismic reflection profile P2 and its interpretation. Location of inset in Fig. 1. Bathymetric data used in inset sourced from Dorschel et al. (2018). Location of IODP Site U1474. TWTT = two-way travel time. MTD = mass transport deposit.

Fig. 4: Core log with downcore variation in bioturbation intensity, grain size (% for D10, D50, D90), magnetic susceptibility (instrument units, ~10^{-5} SI), bulk density (g/cm^3) and P-wave velocity (m/s). In the lithological log, grey represents clay and yellow represents sand. The crosses in the grain size plots denote the location of the samples where measurements were made. The alternating green and pink zones in unit 3 represent the different cycles in P-wave velocity and the magnetic susceptibility logs.

Fig. 5: Age-depth relationships for IODP Site U1474 based on planktonic foraminifera (red circles), calcareous nannofossils (blue circles) and magnetostratigaphy (green triangles) (adapted from (Hall et al., 2017)). Orange lines correspond to the age-depth line for the boundary between units 2 and 3 (dashed), and between units 3 and 4 (solid).

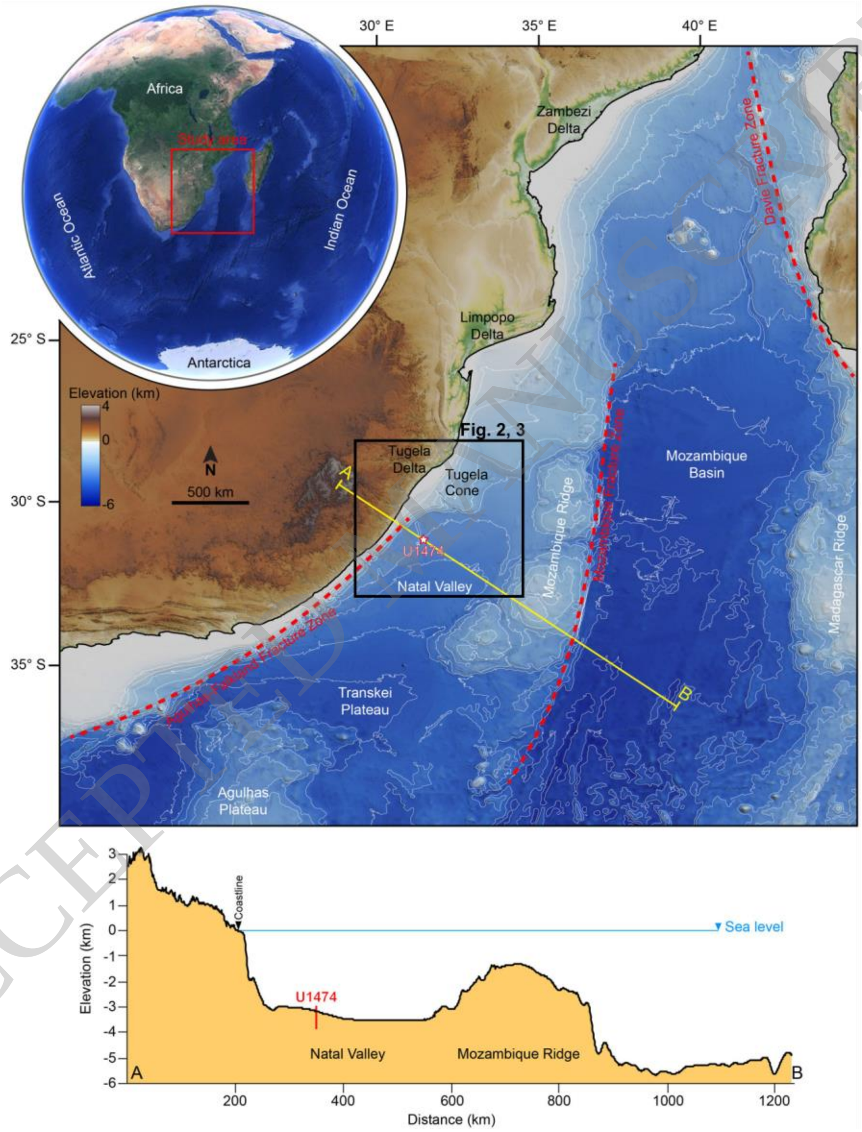
Africa
Study area
Atlantic Ocean
Indian Ocean
Antarctica
30° E
35° E
40° E
25° S
30° S
35° S
Zambezi Delta
Limpopo Delta
Davie Fracture Zone
Elevation (km)
4
0
-6
N
500 km
Fig. 2, 3
Tugela Delta
Tugela Cone
A
U1474
Natal Valley
Mozambique Ridge
Mozambique Fracture Zone
Mozambique Basin
Madagascar Ridge
Agulhas-Falkland Fracture Zone
Transkei Plateau
Agulhas Plateau
B
Elevation (km)
3
2
1
0
-1
-2
-3
-4
-5
-6
Coastline
Sea level
U1474
Natal Valley
Mozambique Ridge
A
B
200
400
600
800
1000
1200
Distance (km)

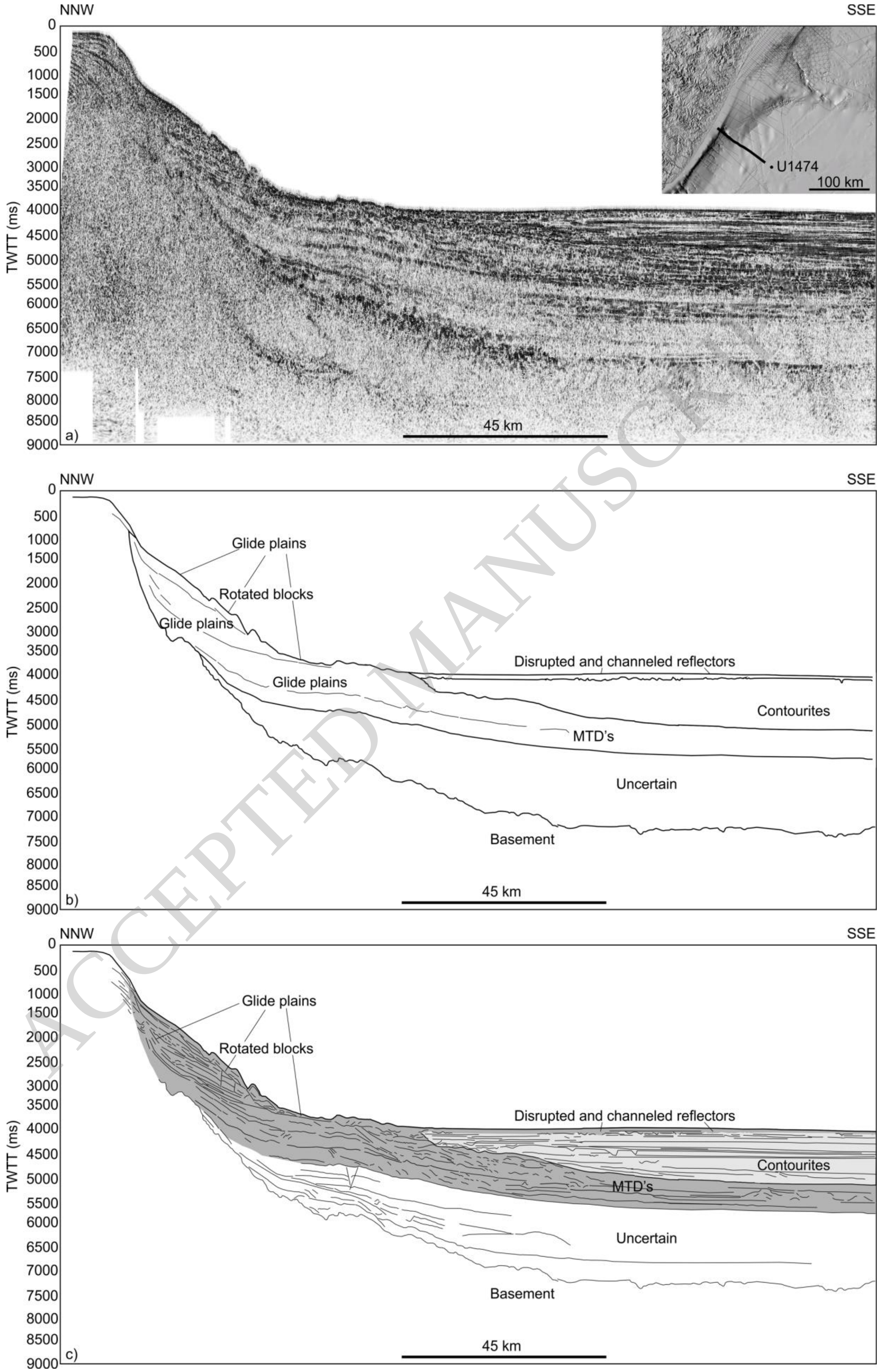
NNW
SSE
TWTT (ms)
0
500
1000
1500
2000
2500
3000
3500
4000
4500
5000
5500
6000
6500
7000
7500
8000
8500
9000
a)
45 km
U1474
100 km
b)
Glide plains
Rotated blocks
Glide plains
Glide plains
Disrupted and channeled reflectors
Contourites
MTD's
Uncertain
Basement
c)
Glide plains
Rotated blocks
Disrupted and channeled reflectors
Contourites
MTD's
Uncertain
Basement

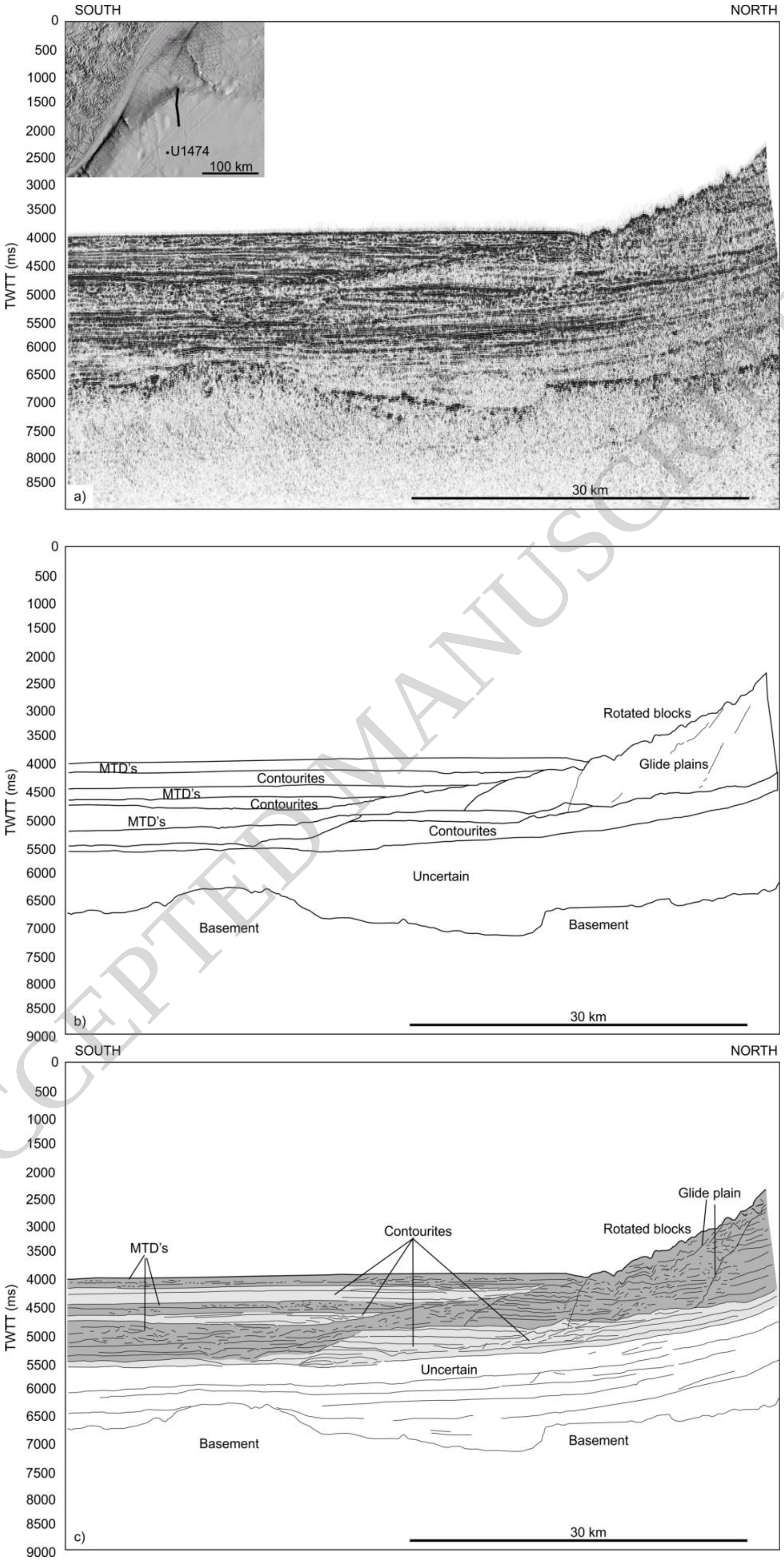
SOUTH
NORTH
TWTT (ms)
0
500
1000
1500
2000
2500
3000
3500
4000
4500
5000
5500
6000
6500
7000
7500
8000
8500
9000
U1474
100 km
a)
30 km
MTD's
Contourites
MTD's
Contourites
MTD's
Contourites
Rotated blocks
Glide plains
Uncertain
Basement
Basement
b)
30 km
MTD's
Contourites
Glide plain
Rotated blocks
Uncertain
Basement
Basement
c)
30 km

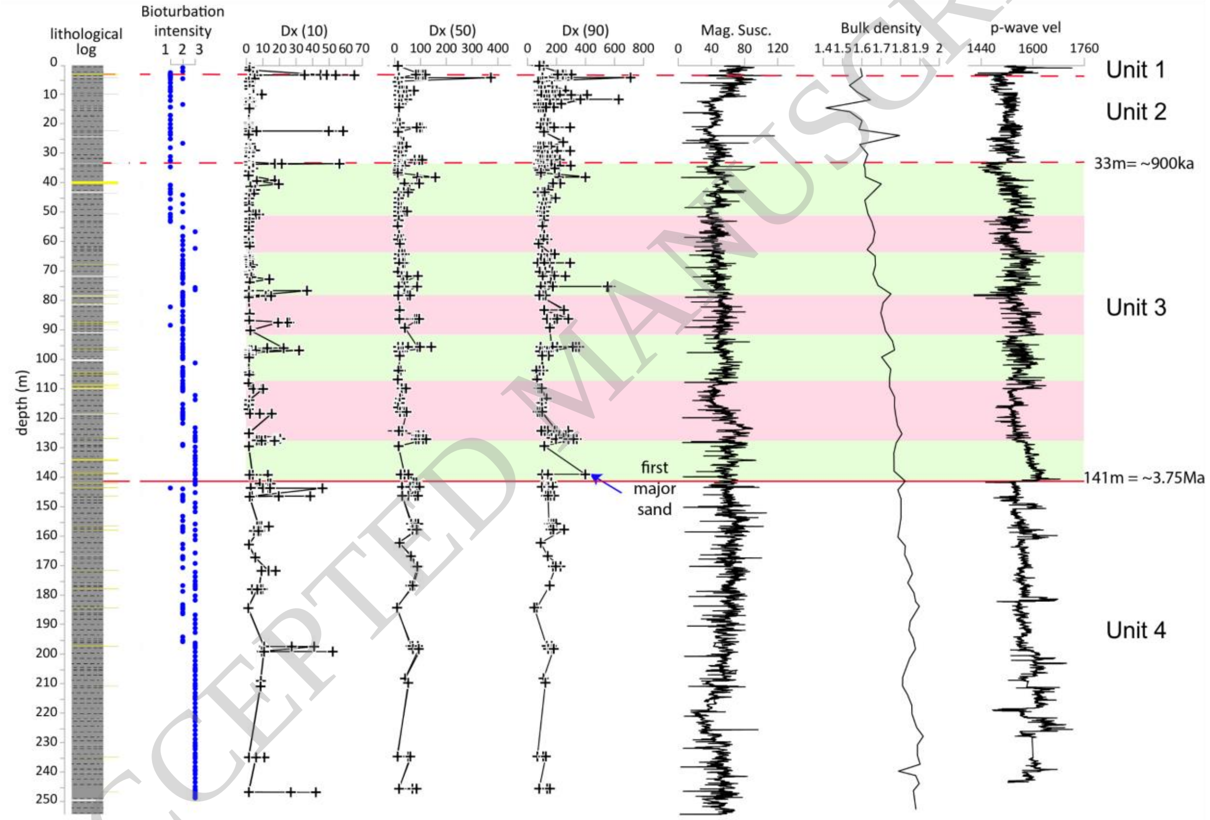
lithological log
Bioturbation intensity
1 2 3
Dx (10)
0 10 20 30 40 50 60 70
Dx (50)
0 100 200 300 400
Dx (90)
0 200 400 600 800
Mag. Susc.
0 40 80 120
Bulk density
1.4 1.5 1.6 1.7 1.8 1.9 2
p-wave vel
1440 1600 1760
depth (m)
0 10 20 30 40 50 60 70 80 90 100 110 120 130 140 150 160 170 180 190 200 210 220 230 240 250
Unit 1
Unit 2
33m= ~900ka
Unit 3
first major sand
141m = ~3.75Ma
Unit 4

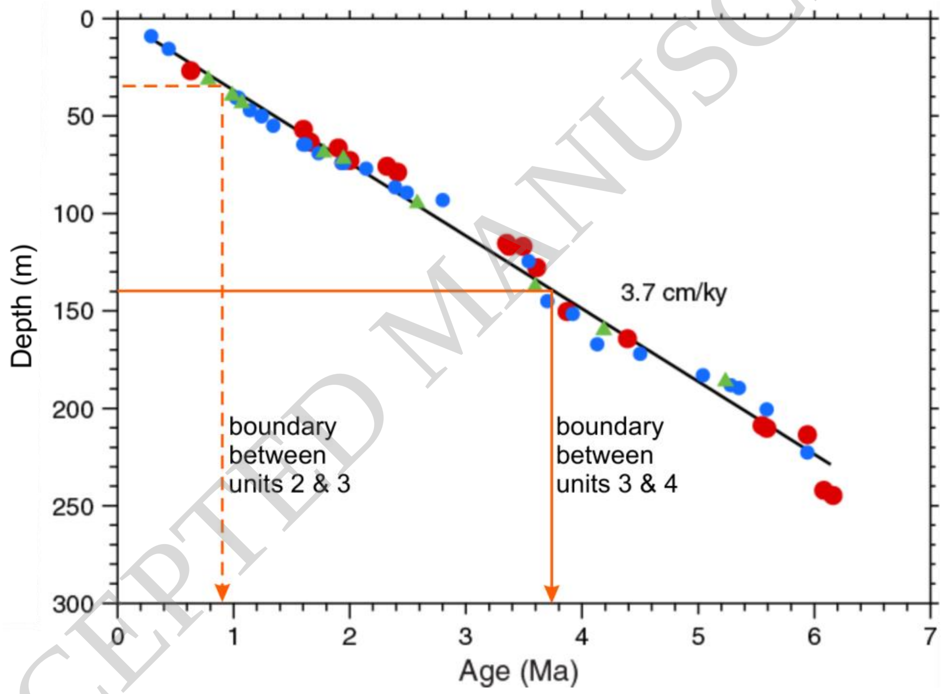
0
50
100
150
200
250
300
Depth (m)
0
1
2
3
4
5
6
7
Age (Ma)
3.7 cm/ky
boundary between units 2 & 3
boundary between units 3 & 4